

Increasing the Accuracy of MDOF Road Reproduction Experiments: Calibration, Tuning and a Modified TWR Approach

F. De Coninck, W. Desmet, P. Sas

K.U.Leuven, Department of Mechanical Engineering,
 Celestijnenlaan 300 B, B-3001, Heverlee, Belgium
 e-mail: Filip.DeConinck@mech.kuleuven.ac.be

Abstract

A CUBE™ high frequency 6-DOF shaker table has recently been installed at the KULeuven Vehicle Technologies Laboratory. This paper describes a dual hardware-software approach for increased accuracy of Multi-Degree-Of-Freedom (MDOF) road reproduction experiments. On the KULeuven 6-DOF high-frequency shaker table, the hardware is calibrated using a mobile Coordinate Measuring Machine (CMM) and both hardware and software settings are tuned for better accuracy. In addition, a modified Time Waveform Replication (TWR) algorithm is presented that yields more stable control and reduction of unwanted rotations.

1 Introduction

Since its installation [1], the CUBE™ 6-DOF shaker table at the KULeuven Vehicle Technologies lab has been used for SDOF shock and vibration testing [2], MDOF Random Vibration Control (RVC) [3, 4] as well as for MDOF road reproduction experiments [5, 6]. These experiments already showed high performance and accuracy over the frequency range 0-300 Hz, results are summarized in Table 1 for the signal rms error (Equation 1) and the Acceleration Spectral Density (ASD) error (Equation 2).

$$\text{Signal RMS error} = \frac{\text{rms}(\text{target}) - \text{rms}(\text{signal})}{\text{rms}(\text{target})} \quad (1)$$

$$\text{Acceleration Spectral Density error (dB)} = 10 \cdot \log \left(\frac{\text{ASD}(\text{signal})}{\text{ASD}(\text{target})} \right) \quad (2)$$

Experiment	Frequency (Hz)	Acceleration (g)	Payload (kg)	RMS error	ASD error (dB)
SDOF RVC	2-300	2 (peak)	150	4.6%	4.8 (max)
MDOF RVC	10-300	0.2 (rms)	30	0.3-3%	2.9 (max)
SDOF Shock	30 ms half sine	5 (peak)	450	-	-
SDOF TWR	5-150	0.6 (rms)	450	2%	2 (max)
MDOF TWR	5-150	3 (peak)	quarter car	3.5%	5.2 (max)

Table 1: Experimental Results

Figure 1 shows some results from the MDOF experiments with the CUBE™ shaker table presented in [6] using TWR software from LMS International [7, 8]. The blue line is the target spectrum from road measurements, the green line the spectrum after eight model updates in the System Identification (SI) step of the

TWR procedure and the red line is the final result spectrum after five iterations in the Target Simulation (TS) step of the TWR procedure. Blue and red curve are closely matched in the frequency band, except for the region 55-85 Hz where larger deviations appear.

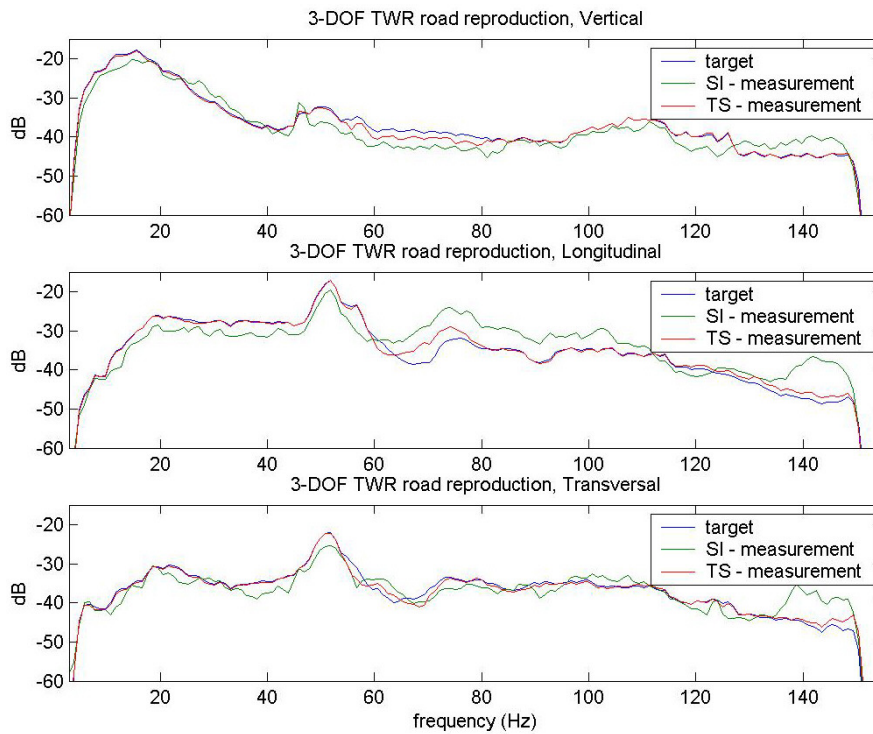


Figure 1: Road reproduction results - spectra

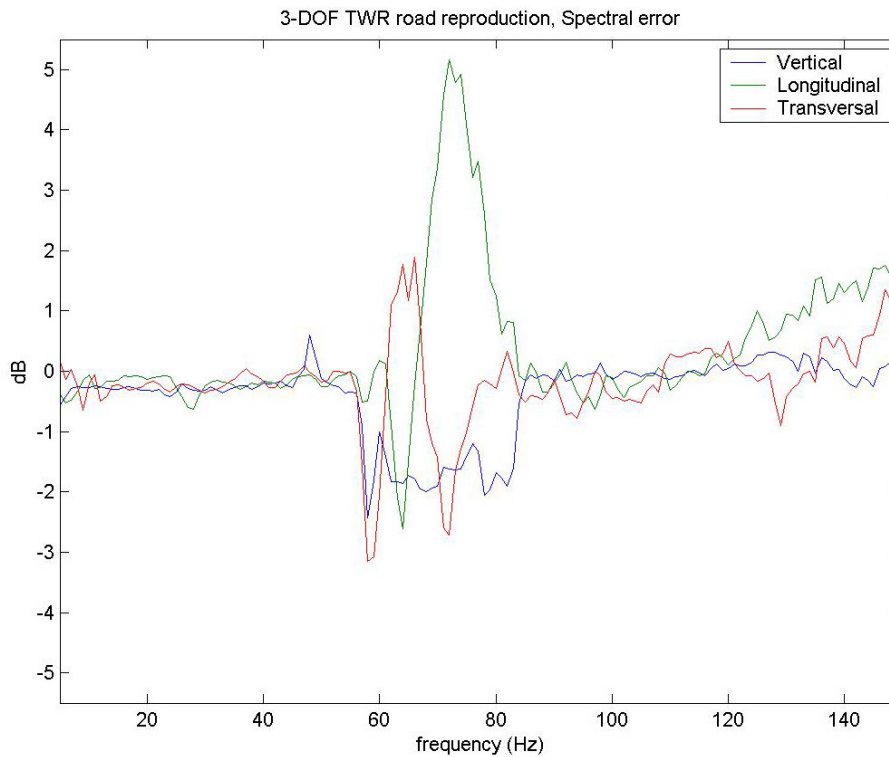


Figure 2: Road reproduction results - spectral error

Figure 2 shows the spectral error curves for the vertical, longitudinal and transversal DOF's (Z,X,Y). The larger errors in the region 55-85 Hz can be clearly distinguished. It is believed by the authors that these larger errors are related to the rotational DOF's of the system, which are in the present applications not controlled by the TWR algorithm, but only by the system's low-level PID controller. These *uncontrolled* rotations transfer energy between the controlled DOF's, causing cross-DOF disturbances in the TWR algorithm. This paper reports on a calibration and tuning approach that reduces those cross-DOF disturbances.

Following this introduction, the second section discusses the shaker concept along with the mechanism that causes cross-DOF energy flows through unwanted rotations. For further analysis a 2-DOF (Z, Pitch) simulation model is built in Matlab Simulink. In the third section the calibration and tuning parameters and their influence on the system performance and accuracy are explained. The fourth section introduces the modified TWR approach, while in the fifth section simulation results from the 2-DOF Simulink model are presented.

2 The CUBE™ shaker concept

2.1 The integrated shaker

The CUBE™ shaker table is quite revolutionary by its fully integrated concept. In contrast with a conventional hydraulic test system, the six integrated actuators are located on the inside. Figure 3 shows on the left the inside arrangement and numbering of the actuators, on the right a look-through scale model on the foreground and the actual shaker in the background. The red arrows indicate the mapping of the actuators between the inside schematic and the scale model. Each orthogonal direction (X-Y-Z) has two actuators in a parallel configuration, further referenced as an actuator pair.

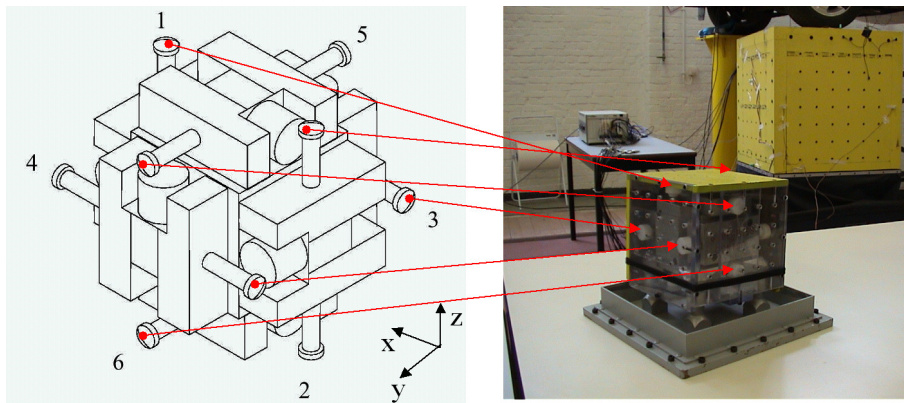


Figure 3: Integrated shaker arrangement

Each single actuator consists of two hydraulic pistons, with the high performance two-stage "voice-coil driven" servo valves located in between. Each piston is used for a single direction of motion, with the magnesium outer shell connecting the pistons, such that they move as one entity and thus closing the kinematical chain. Hydrostatic bearings are used for the piston and the piston head, resulting in almost frictionless operation. An LVDT position sensor is attached to one of the piston heads of each actuator. Locating the hydraulic valves in between both pistons, reduces the hydraulic path to a strict minimum and thus increases the bandwidth of the shaker system. The valve's second stage spool position is measured by the valve LVDT. The six degrees of freedom are realized by jointly or oppositely driving the three actuator pairs. There is one pair for each orthogonal direction, with two degrees of freedom, one translation and one rotation, for each pair.

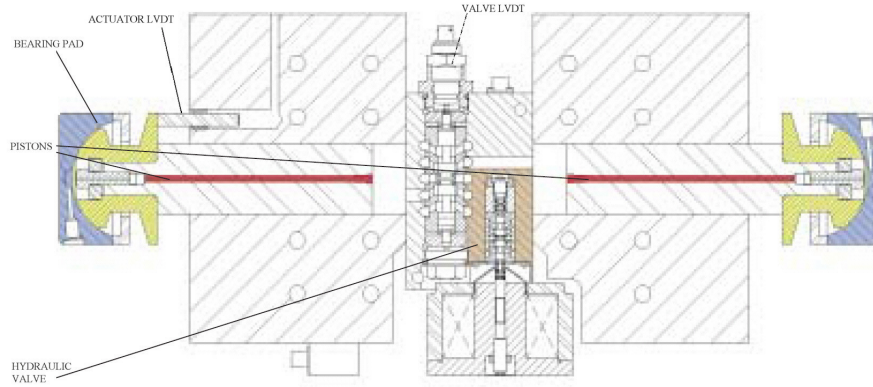


Figure 4: Actuator configuration and components

2.2 The concept of modal control

In the standard control configuration, called "non-modal", all six shaker actuators can be controlled individually. However, to achieve a translation or rotation, two actuators of a pair need to be combined. In order to execute a SDOF translation, both actuators of the concerned orthogonal direction receive the same driving signal. If both actuators respond equally, an identical translation in both actuators is generated and the shaker table executes a perfect translation (Figure 5a shows this for Z-translation). For a SDOF rotation, both actuators receive the same amplitude of driving signal, but with opposite sign. If both actuators respond equally, a rotation of the shaker table is induced (Figure 5b shows this for Y-rotation or Pitch). The transformation from actuator DOF's to modal DOF's is defined by equations 3 and 4 for Z and Pitch displacement:

$$Z = \frac{actuator_1 + actuator_2}{2} \quad (3)$$

$$Pitch = \frac{actuator_1 - actuator_2}{2} \quad (4)$$

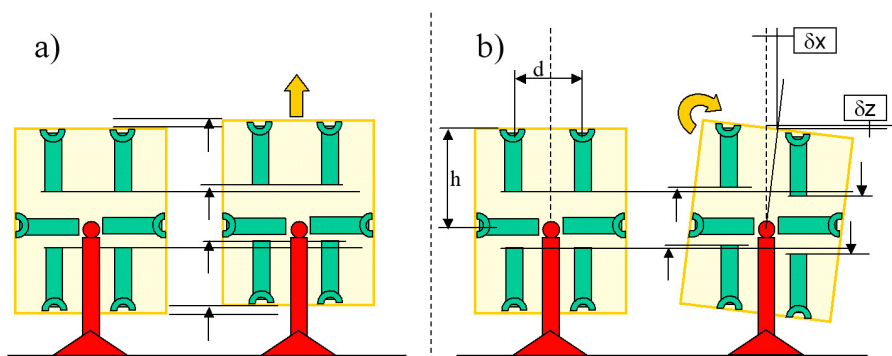


Figure 5: SDOF Translation (a) and Rotation (b)

As can be seen in Figure 5b the rotation around the Y-axis (Pitch) induces secondary effects at the table top center: a large X translation (δX) and a small Z translation (δZ). These values, for small Pitch displacements, are approximated by the equations 5 and 6:

$$\delta Z = h \cdot (1 - \cos(\alpha)) \quad (5)$$

$$\delta X = h \cdot (\sin(\alpha)) \quad (6)$$

with the pitch angle α , for small rotations approximated by:

$$\alpha = \arcsin\left(\frac{2 \cdot Pitch}{d}\right) \tag{7}$$

which yields for δX

$$\delta X = h \cdot \left(\sin\left(\arcsin\left(\frac{2 \cdot Pitch}{d}\right)\right)\right) = h \cdot \frac{2 \cdot Pitch}{d} \tag{8}$$

with h the distance between the horizontal actuator centerline and shaker table top and with d the centerline distance between two actuators of the same pair. For small rotations the δZ values are very small and can be compensated for in the Z control loop, as they are observable (Z-sensor) and controllable (Z-actuator). The δX values however are more important. With typical X target levels at 50% of Z target levels, unwanted Pitch levels around 0.5 - 1.5% of the Z target and h/d about 1, δX values can become dominant for the X-DOF accuracy. These errors are (indirectly) observable if they are caused by the Z-drive, through the $X_{response}/Z_{drive}$ FRF: H_{XZ} . The cross-DOF FRF's (H_{XZ} , H_{ZX}) are generally less accurate than the diagonal FRF's (H_{ZZ} , H_{XX}) as is explained in section 4. Considerable cross-DOF influence therefore exists in a conventional control system, causing the need to actively control the rotational DOF's to zero.

2.3 A 2-DOF Simulink model

A 2-DOF model for the Z and Pitch DOF's of the shaker table is built in Matlab-Simulink (Figure 6). This model is based on a 2-DOF state-space (linearized) model (green) of the system represented in Figure 5, with shaker mass, rotational inertia, hydraulic damping (viscous) and hydraulic stiffness (constant K). This block is preceded by a valve-block (yellow), representing the dynamics of the voice coil valves. The software PID loop (blue) and modal transformation (red) constitute the top level of the model. This model is used to implement the different calibration and tuning issues discussed in section 3 for the evaluation of the modified TWR algorithm.

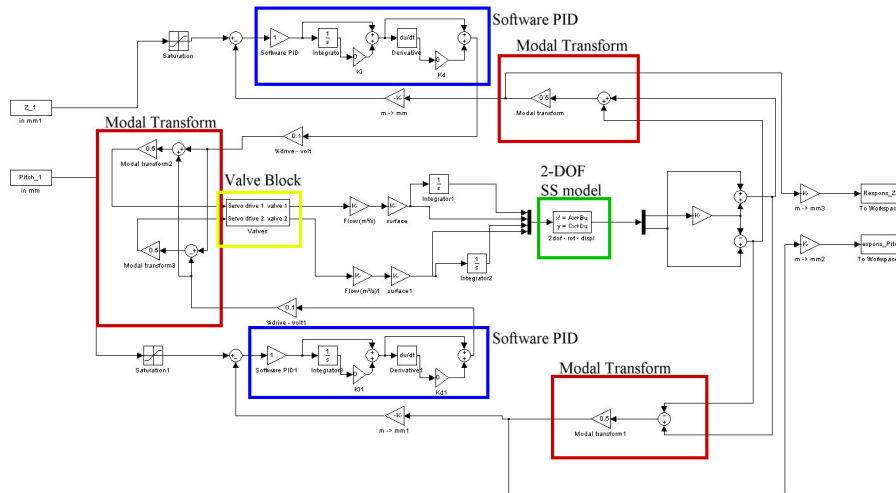


Figure 6: Simulink model for Modal 2DOF system

3 Calibration and tuning parameters

Calibration and tuning is generally performed by the manufacturer of the hydraulic test system (partially) before and (partially) after installation at the customers site. Standard procedures and specifications exist

[9, 10, 11] and are more than sufficient for general customer requirements, as can be concluded from Table 1 and the 6-DOF signal rms error of 5-10% mentioned in [12]. The specific use of the shaker at the KULeuven lab for system identification purposes sharpens these requirements ($\approx 0.5-1\%$ signal rms accuracy) and creates the need for more accurate on-site calibration and tuning procedures.

3.1 The hydraulic environment

The hydraulic environment, consisting of the hydraulic pump and oil tank, is generally not considered as a tunable unit in hydraulic test systems. These elements however are crucial to the optimal performance of the global system. It was experienced at the KULeuven lab that the hydraulic shaker (in light of the desired accuracy) is remarkably sensitive to the pressure settings, oil cleanliness and oil temperature. It is a misunderstanding that such parameters can be compensated for in software. An example for each parameter is given to illustrate that this is not the case. Inaccurate settings lead to bad performance or high-levels of signal noise, none of which can be compensated for in software:

- Oil cleanliness: very thorough filtering was performed at the KULeuven site to achieve a far better cleanliness level than required. This results in less particles disturbing the operation of the servo-valve and thus less hydraulic noise,
- Oil pressure: the use of hydrostatic bearings yields an almost frictionless operation. If the system pressure is set too high, the leaking flow through the bearing clearance changes from laminar to turbulent flow, resulting in higher signal noise levels. The pressure setting on the KULeuven shaker was tuned to maximize performance under low-noise conditions. About 15% of peak performance was sacrificed for this.
- Oil Temperature: The viscosity of the hydraulic oil is function of temperature. This viscosity is also determining the location of the laminar-turbulent flow transition, which causes repeatability errors. Because of the pressure setting tuned relatively close to this transition, temperature variations need to be kept within $\pm 5^\circ$ Celsius. Normal system (\neq local oil temperatures) temperature variations are about $\pm 10^\circ$ Celsius.

None of the above mentioned errors can be compensated for in software, as they are stochastic in nature and not repeatable over several iterations. Error levels can vary from lower than 1% to more than 15% signal rms depending on the settings of the hydraulic power supply and oil cleanliness.

3.2 Valve span matching

The voice coils of the hydraulic valves are mechanically centered using steel springs. In order to center the valve zero-flow point with regard to the zero valve drive point, a voltage offset is added to the valve drive signal. In this way, the software dynamic range is centered with regard to the hardware dynamic range center. The span setting on the system valves is used as a gain on the servo-valve position feedback before it enters the comparator with the valve drive signal. This is necessary to enable the voltage offset. Valves belonging to the same actuator pair are given the same span setting. This assumes the valve spool LVDT's on both valves to be accurately calibrated. No on-site verification or calibration procedure for the valve spool LVDT's is available. Span mismatch is not very detrimental for the accuracy of low frequency experiments ($<50\text{Hz}$) because of the faster dynamics of the valve control loop and can to a large extent be compensated for in software at higher frequencies, as long as the resulting motion or error occurs in an observable DOF and is directly controllable (same DOF). It is explained in section 4 that this cannot always be implemented due to stability issues of the standard TWR algorithm. Extra errors to compensate for also use up some of the (limited) available updating loops. Span matching on the KULeuven shaker was performed up to (quasi-) perfect matching.

3.3 Valve dynamics matching

The servo-valve hardware control loop is tuned by a proportional gain. Standard tuning procedures match the amplitude response of valves belonging to the same actuator pair at a single given frequency, usually the 90° phase shift point. On most systems this parameter is not allowed to be tuned on-site, as it is done in the factory by specialized personnel in the valve workshop.

At the KULeuven lab, the frequency response functions of the two valves are measured in the range 0-300Hz for a white noise valve drive signal. Response curves are overlaid for amplitude and phase and tuning is performed for the best overall matching of the valves. This procedure is by far more time consuming and requires detailed analysis of the amplitude and phase plots. Significant accuracy improvements can be achieved by tuning this parameter as is shown in section 5. The gain setting is limited by the dynamics of the valve control loop. Each gain setting is checked using square wave signals according to the PID tuning procedure explained in 3.6.

3.4 Sensor calibration



Figure 7: Krypton K600 Mobile CMM camera system

The position of each actuator is measured by an LVDT sensor. Calibration of this sensor is necessary to achieve correct displacement and rotation readout. A small calibration mismatch between two actuators of a single pair leads to unwanted rotations. Suppose actuator₁ and actuator₂ have respectively +1% and -1% calibration error. For a pure vertical displacement, the modal coordinate Z will have 0% error (equation 3), but the Pitch will have 1% error (equation 4). In order to remove this error, the pitch PID controller will rotate (pitch) the shaker by 1% proportional to the Z displacement. These rotations can excite the hydraulic resonances [1, 13, 14] and seriously disturb TWR experiments if the pitch is not actively controlled. Even with active control of the pitch DOF, signal levels of the (unwanted) rotations and cross-DOF generated errors are still in the range of the Z tracking accuracy (see section 2.2).

Sensor calibration on the shaker table is performed using a mobile CMM, a K600 camera system from Krypton (Figure 7), which measures the motion of the shaker table during a specific calibration sequence [15, 16]. Tracking is recorded on both the LVDT sensors and the K600 system. A custom algorithm in Matlab is used to compare both measurements, estimate the noise levels and calculate the required calibration corrections.

3.5 Offset removal

As discussed in 3.4, the position of each actuator is read by an LVDT sensor. The LVDT is originally calibrated during the assembly of the shaker with gage blocks. After assembly of the outer shell, it is possible that an offset exists between the symmetry center of the inner structure and thus the actuator force center, and the outer shell geometric and mass center. A translation force by the actuators will, by means of the offset, also generate a torque on the outer shell and induce a rotation. The amount of offset depends on the machining and assembly tolerances, the sensor calibration and the software offset parameter. Sensor offsets can cause problems and need to be verified and if necessary removed. This can be done by centering the outer shell around the shaker's displacement stop blocks, assuming that they are symmetrical with regard to the actuators, or by using the K600 system mentioned above.

3.6 PID tuning

PID-tuning is considered as a key task in the search for more accuracy [8, 17]. It is true that TWR software can compensate to some extent for, mostly less dynamic, PID tuning. TWR experiments however are sensitive to the phenomenon called over-iteration. The number of iteration steps with increasing accuracy is limited and followed by steps with decreasing accuracy and sometimes overcompensation and stability issues.

Desirable PID settings yield, for a square wave tuning signal, a maximum of 5% overshoot, minimal rise time, low tracking error and no oscillations. For the PID tuning the shaker table is put in a "neutral" position where the force center and mass center coincide. A specific parameter for hydraulic systems is the dither, a high-frequent oscillation, permanently applied to keep the valve spool clean and moving. Because of the high-dynamic range of the shaker table, with considerable dynamic response up to 500Hz and beyond, dither frequency is set at 1250Hz. An advantage of having very clean oil in the system, is that very low dither settings can be used, compared to standard practice, with lower disturbance for the measurements and operator.

4 A modified TWR algorithm

Next to calibration and tuning of the hardware and software, as discussed in section 3, a modified TWR algorithm is presented in this paper. The need for a more accurate and stable algorithm is based on the authors' experience with MDOF road reproduction experiments, as presented in the introduction. For the specific case of experiments with only translational targets (=rotational targets equal to zero) larger spectral errors were recorded in the 55-85Hz frequency range (see Figure 2). It is believed by the authors that the larger errors are related to the rotational DOF's of the system, which are in the present applications not controlled by the TWR algorithm, but only by the system's low-level PID controller.

4.1 The standard TWR approach

Time Waveform Replication is an advanced implementation of the off-line feedforward control strategy for a system with N input drives (= controlled DOF's) and M (= observed DOF's) output signals ($M \geq N$). N and M can be chosen less than the maximum DOF's of a system, the *uncontrolled* DOF's are then only handled by the system's low level PID-controller, with target equal to zero. The TWR procedure is split up in a System Identification (SI) step and a Target Simulation (TS) step. In the SI step, uncorrelated white or filtered noise on all input drives is used to estimate the systems FRF matrix $H(\omega)$. Equation 9 shows this for the 2-DOF (Z, Pitch) model:

$$\begin{bmatrix} Z(\omega)_{signal} \\ Pitch(\omega)_{signal} \end{bmatrix} = \begin{bmatrix} H(\omega)_{ZZ} & H(\omega)_{ZPitch} \\ H(\omega)_{PitchZ} & H(\omega)_{PitchPitch} \end{bmatrix} \cdot \begin{bmatrix} Z(\omega)_{drive} \\ Pitch(\omega)_{drive} \end{bmatrix} \quad (9)$$

In the SI step, further refinement of $H(\omega)$ can be achieved by updating the drives until the signal spectra match closely with the target spectra. The aim is to improve the model accuracy by being less sensitive to amplitude non-linearities. A better model yields more accuracy in the TS step. With the refined $H(\omega)$ the TS step is started with the first drive (equation 10), followed by a (limited) number of updating loops (equation 11). C_1 and C_2 are user defined updating constants, typically 50-80%.

$$\begin{bmatrix} Z_{drive}^1 \\ Pitch_{drive}^1 \end{bmatrix} = C_1 \cdot H^{-1} \begin{bmatrix} Z_{target} \\ Pitch_{target} \end{bmatrix} \quad (10)$$

$$\begin{bmatrix} Z_{drive}^{i+1} \\ Pitch_{drive}^{i+1} \end{bmatrix} = \begin{bmatrix} Z_{drive}^i \\ Pitch_{drive}^i \end{bmatrix} + C_2 \cdot H^{-1} \left(\begin{bmatrix} Z_{target} \\ Pitch_{target} \end{bmatrix} - \begin{bmatrix} Z_{signal}^i \\ Pitch_{signal}^i \end{bmatrix} \right) \quad (11)$$

For a 2-DOF system, with one translation and one rotation, as developed for the simulation model, three TWR system configurations for a pure translation target can be used:

- The non-modal 2-DOF system: both actuators of the system receive the same target (Figure 8, Equation 12)

$$\begin{bmatrix} Act1(\omega)_{signal} \\ Act2(\omega)_{signal} \end{bmatrix} = \begin{bmatrix} H(\omega)_{11} & H(\omega)_{12} \\ H(\omega)_{21} & H(\omega)_{22} \end{bmatrix} \cdot \begin{bmatrix} Act1(\omega)_{drive} \\ Act2(\omega)_{drive} \end{bmatrix} \quad (12)$$

- The modal 2-DOF system: the translational DOF receives the target signal, the rotational DOF receives a zero target (Figure 9, Equation 9)
- The modal 1-DOF system: only the translational DOF is included in the system (Figure 10, Equation 13)

$$[Z(\omega)_{signal}] = [H(\omega)_{ZZ}] \cdot [Z(\omega)_{drive}] \quad (13)$$

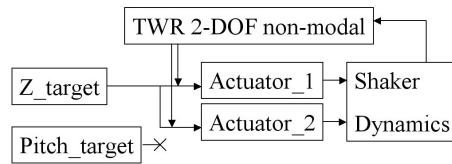


Figure 8: The non-modal 2-DOF system

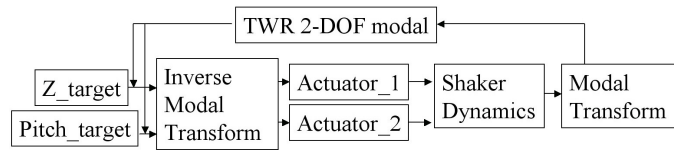


Figure 9: The modal 2-DOF system

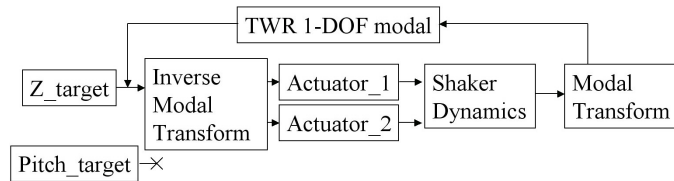


Figure 10: The modal 1-DOF system

All three approaches feature drawbacks, that in the scope of the desired accuracy can be considered as significant. The non-modal approach is very sensitive to differences in dynamic response from the actuators. This already starts in the SI step, where uncorrelated white or filtered noise is used, yielding slightly different transfer functions for identical actuators. Due to this, rotations are generated during the first drive of the TS step. These rotations cannot be controlled to be lower than the translation accuracy, because in the minimization formula of the algorithm (14) translation and rotation errors are treated in the same way:

$$error^i = \sqrt{(Act1_{target} - Act1^i_{signal})^2 + (Act2_{target} - Act2^i_{signal})^2} \quad (14)$$

The modal 2-DOF system is in theory best suited to achieve high accuracy in both translation and rotation DOF (for example Z and Pitch). The configuration works very well for applications where significant energy is present in both translation and rotation target signals. However, for applications where the rotational DOF needs to be controlled to zero, as is the case here, the TWR algorithm experiences stability issues. The

system is identified with uncorrelated noise on both DOF's, resulting in a 2x2 FRF matrix. The off-diagonal FRF's are small, and, relative to the diagonal terms, inaccurate. The first problems occur when target shaped noise is used to update the FRF model. The first time, a zero signal is used for the Pitch, but this leads to very bad identification of all the FRF's except the Z_{drive} to $Z_{response}$ FRF (H_{ZZ}). The other three FRF's used to create the next Pitch (and part of the Z) drive are now very inaccurate and the Pitch drive is unacceptably amplified in the next update. The possibility exists to use the first model for the target simulation, as is done in the Matlab model, but the reproduction result is unavoidably less accurate.

The modal 1-DOF system is in practice the most suited for these experiments. Only one driving signal is equally fed to both actuators, yielding for a perfect system, a rotation free response. Stability is guaranteed in all circumstances because of the high accuracy of the FRF (1x1) and the level of energy in this DOF. System inaccuracies, as discussed in 3, cause unwanted rotations, which are not observable nor controlled by the TWR algorithm. Rotations are only observed and controlled by the system's low-level PID controller.

4.2 The modified TWR approach

The modified approach is based on the idea of decoupling the two DOF's and updating them separately in a 2-stage TWR algorithm (Figure 11, Equation 15).

$$\begin{bmatrix} Z(\omega)_{signal} \\ Pitch(\omega)_{signal} \end{bmatrix} = \begin{bmatrix} H(\omega)_{ZZ} & 0 \\ 0 & H(\omega)_{PitchPitch} \end{bmatrix} \cdot \begin{bmatrix} Z(\omega)_{drive} \\ Pitch(\omega)_{drive} \end{bmatrix} \quad (15)$$

The first step in the decoupling is achieved by minimizing the off-diagonal FRF's of the 2-DOF system

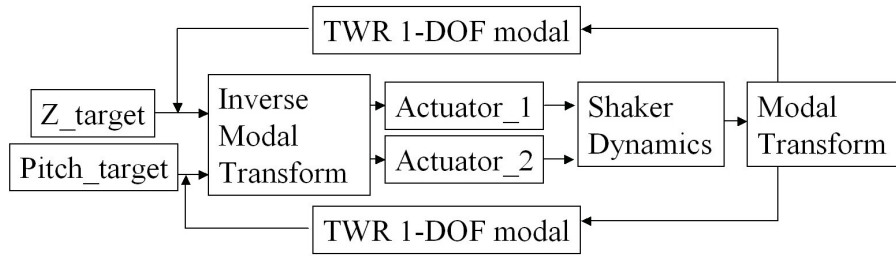


Figure 11: The modal 1(+1)-DOF system

through calibration and tuning as discussed in 3. This is necessary to minimize the cross-DOF influences of the separate loops so that the system behavior can be approximated by equation 15. Next, the stability problems of the 2-DOF modal configuration are tackled by splitting it up in a 1(+1)-DOF system. In fact, two 1-DOF TWR routines are running alternatively. First the 1x1 FRF is identified for both DOF's (Equation 16). Next the procedure of the modal 1-DOF(Z) system is started until signal levels are at about 75-90% of the Z target (Equation 17,18). At this point updating loops of the Z and Pitch 1-DOF TWR system are run sequentially (Equation 18,19), with a 2-DOF drive used for every loop, but only one of the two drives updated per loop. When Z accuracy is acceptable, one or two Pitch-only loops (Equation 19) are performed to further decrease the rotations.

$$[Z(\omega)_{signal}] = [H(\omega)_{ZZ}] \cdot [Z(\omega)_{drive}] , [Pitch(\omega)_{signal}] = [H(\omega)_{PitchPitch}] \cdot [Pitch(\omega)_{drive}] \quad (16)$$

$$[Z_{drive}^1] = C_1 \cdot H_{ZZ}^{-1} [Z_{target}] \quad (17)$$

$$[Z_{drive}^{i+1}] = [Z_{drive}^i] + C_2 \cdot H_{ZZ}^{-1} \left([Z_{target}] - [Z_{signal}^i] \right) \quad (18)$$

$$[Pitch_{drive}^{j+1}] = [Pitch_{drive}^j] + C_2 \cdot H_{PitchPitch}^{-1} \left([Pitch_{target}] - [Pitch_{signal}^j] \right) \quad (19)$$

5 Simulation results

Simulations were performed for six different shaker conditions : perfect (Model B), valve span mismatch (5%) (Model C), valve gain mismatch (5%) (Model D), calibration error (5%) (Model E, TWR based on real position feedback, real position error), calibration error (5%) (Model E', TWR based on sensor position feedback, sensor position error¹), offset error (5%) (Model F) and for four control system configurations : 2-DOF non-modal, 2-DOF modal, 1-DOF modal and the modified 1(+1)-DOF modal algorithm, referenced to as the 2-stage TWR. For the first three configurations, one identification and eight updates are performed, for the last system one identification in parallel and a total of thirteen alternative updates has been run, eight for translation and five for rotation.

Simulation results for a Z sine wave target (5 Hz, 1 mm amplitude) are shown in Figure 12a and Figure 12b for the Z and Pitch error respectively.

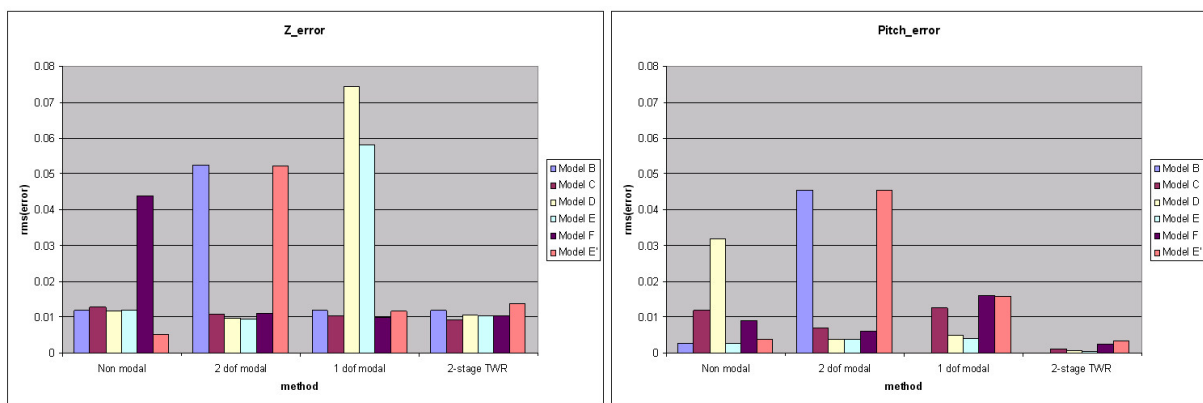


Figure 12: Sine wave target, relative rms(error): Z (a:left) and Pitch (b:right)

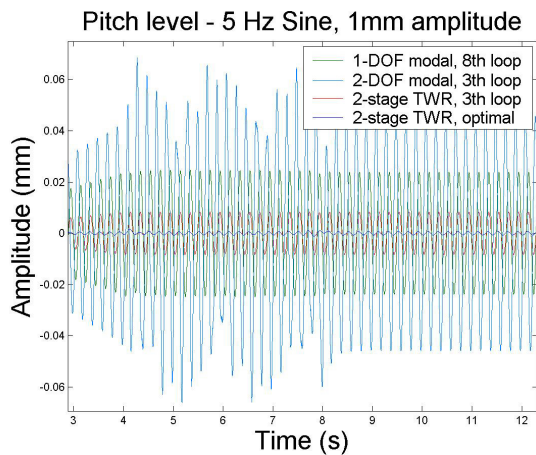


Figure 13: Pitch levels for a Z target of 5Hz, 1mm

The modified approach does not deliver the best Z accuracy in every case, but differs from the lowest rms(error) of about 1% by 0.04 to 0.11% rms(error). An exception occurs for model E' where the non-modal approach is about two times better than the others (rms(error) = 0.5%). The 2-stage approach yields the lowest Pitch errors in all simulation cases reducing these Pitch errors with a factor 2.5 to 7 with respect to the second best algorithm. Reduction factors of 6.5 to 47 are seen compared to the worst algorithm. For the different shaker conditions, each standard TWR system configuration (2-DOF non modal, 2-DOF modal, 1-DOF modal) is the worst algorithm at least once. Figure 13 shows a time signal comparison (model F) for the 1-DOF modal (green), 2-DOF modal (cyan), a 2-stage TWR (red) with only sequenced updating loops and a 2-stage TWR (blue) as described above. The 2-DOF system has an unstable Pitch response, the 1-DOF system a stable but uncontrollable Pitch response. The 2-stage TWR algorithm drastically reduces the unwanted Pitch rotations.

Simulation results for a Z road recording target (0-50 Hz, 1.6 mm rms, 5.5 mm peak) are shown in Figure 14a and Figure 14b for the Z and Pitch error respectively.

¹Even for a zero Pitch sensor error, the real Pitch RMS error is 1.77% of the Z target level for a sine wave target

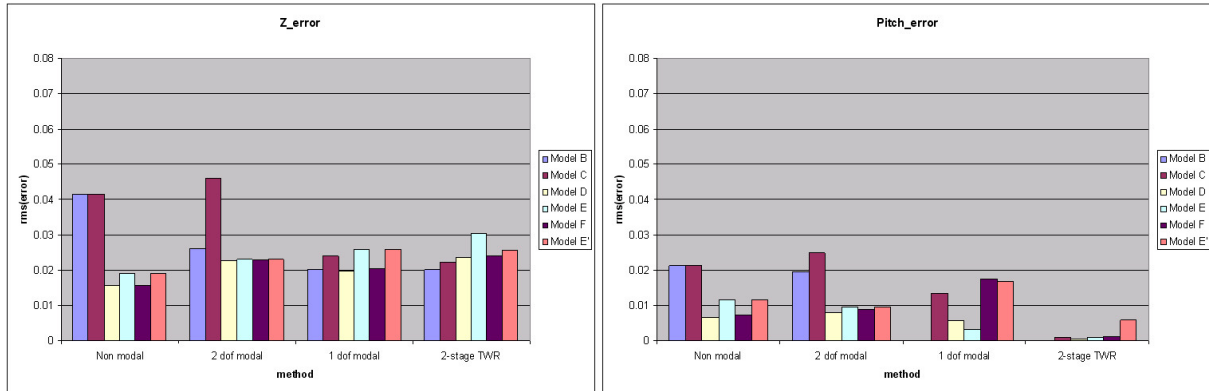


Figure 14: Road recording target, relative rms(error): Z (a:left) and Pitch (b:right)

For this target signal, the modified approach does not deliver the best Z accuracy in every case, but differs from the lowest rms(error) of about 1.5-2.2% by 0.8 to 1.1% rms(error). The 2-stage approach yields the lowest Pitch errors in all simulation cases reducing these Pitch errors with a factor 1.6 to 16.8 with respect to the second best algorithm. Reduction factors of 2.9 to 31 are seen compared to the worst algorithm. For the different shaker conditions, each standard TWR system configuration (2-DOF non modal, 2-DOF modal, 1-DOF modal) is the worst algorithm at least once.

6 Conclusions

In this paper a dual hardware-software approach for increased accuracy of MDOF road reproduction experiments is presented. On the KULeuven MDOF High-Frequency shaker table, the hardware is calibrated using a mobile CMM-system and both hardware and software settings are tuned for better accuracy. In addition, a modified algorithm is presented that yields more stable control and reduction of unwanted rotations. The presented work is not intended for application on all hydraulic experiments or test-systems, but only for MDOF systems running high-accuracy reproduction (road/air/space) experiments. The calibration and tuning yields great benefits for stability, controllability and repeatability, with no implications on test complexity. The modified TWR algorithm requires a 50-75% (time) effort increase for better accuracy and more robust control of unwanted rotations. Next to the experiments on the CUBE™ shaker, fourposter and multi axial shaker tables can benefit considerably from the new approach in case of high accuracy experiments. It was shown that standard tuning, calibration and TWR routines exceed standard customer and test requirements, but are insufficient for the specific high accuracy needs at the KULeuven lab. A significant effort is required in setup and during test to achieve this high accuracy, which makes the presented procedures only suitable if specifically required.

7 Acknowledgements

This research is sponsored by the Belgian programme on Interuniversity Poles of Attraction, initiated by the Belgian State, Prime Minister's Office, Science Policy Programming (IUAP). The research work of Filip De Coninck is financed by a scholarship of the Institute for the Promotion of Innovation by Science and Technology in Flanders (IWT). The authors would like to acknowledge the financial support of the Fund for Scientific Research - Flanders (Belgium) (F.W.O. - Vlaanderen) for the acquisition of the CUBE™ shaker table.

References

- [1] F. De Coninck, W. Desmet, P. Sas, *Installation and Performance Testing of a High Frequency 6-DOF Shaker Table*, RUG, *Proceedings of the National Congress on Theoretical and Applied Mechanics, Ghent, Belgium, 2003 May 26-27*, Ghent (2003), (CD-rom)
- [2] F. De Coninck, W. Desmet, P. Sas, D. Vaes, *Multisine Shock and Vibration Testing using a High-Frequency 6-DOF Shaker Table*, Congrex, *Proceedings of ICSV10, Stockholm, Sweden, 2003 July 7-10*, Stockholm (2003), pp. 1205-1212
- [3] B. Peeters, J. Debillé, F. De Coninck, *Multi-Axial Random Vibration Testing: A Six Degrees-Of-Freedom Test Case*, The Aerospace Corporation, *Proceedings of the 21st Aerospace Testing Seminar, Manhattan Beach, CA, 2003 October 21-23*, Los Angeles (2003), pp. 4.47-4.62
- [4] B. Peeters, J. Debillé, F. De Coninck, *Multi-Shaker Control To Create A Six Degrees-Of-Freedom Vibration Environment*, SAVIAC, *Proceedings of the 74th Shock and Vibration Symposium, San Diego, CA, 2003 October 27-31*, San Diego (2003), (CD-rom)
- [5] F. De Coninck, D. Vaes, J. Swevers, W. Desmet, P. Sas, *Non-Linear MDOF Vehicle Suspension Testing*, SME, *Proceedings of IMAC XXII, Dearborn, MI, 2004 January 26-29*, Dearborn(2004), (CD-rom)
- [6] F. De Coninck, D. Vaes, J. Swevers, W. Desmet, P. Sas, *Vehicle Suspension and Structure Borne Road Noise Testing on a 6-DOF High Frequency Shaker Table : First Outlines*, FISITA, *Proceedings of the 2004 World Automotive Congress, Barcelona, Spain, 2004 May 23-27*, Barcelona (2004), (CD-rom)
- [7] J. De Cuyper, M. Verhaegen, *State Space Modeling and Stable Dynamic Inversion for Trajectory Tracking on an Industrial Seat Test Rig*, Sage Science Press, *Journal of Vibration and Control*, 2002 issue 8, pp. 1033-1050
- [8] S. Vanlanduit, P. Verboven, P. Guillaume, B. Cauberghe, G. Van der Linden, *Towards accelerated endurance testing*, SME, *Proceedings of IMAC XXII, Dearborn, MI, 2004 January 26-29*, Dearborn(2004), (CD-rom)
- [9] J. Davis, *CUBE Facility Preparation*, Team Corporation, *Application Note #CUBE-002*, Seattle, WA, Seattle(2000)
- [10] J. Davis, *Hydraulic Fluid Requirements for Team Hydraulic Systems*, Team Corporation, *Application Note #GEN-0001*, Seattle, WA, Seattle(2000)
- [11] Instron Schenk, *Hydraulic Power Packs, Type PP-BA*, IST Systems GmbH, *Hydropuls Specification 2 PP-BA 9803*, Darmstadt, Germany Darmstadt(1998)
- [12] K. McIntosh, J. Davis, *Multi-axis testing of Under Wing and Ground Vehicle Weapons Systems*, UK & International Press, *Aerospace Testing International*, 2002, July issue
- [13] Team Corporation, *Oil column resonance de-mystified*, Team Corporation, *Team newsletter 2*, Seattle, WA, Seattle(2002)
- [14] F. De Coninck, S. Tollens, *Design and Construction of a Testrig for Brake Judder Analysis*, KULeuven, *Master Thesis, Leuven, Belgium*, Leuven(2001), pp. 53-54
- [15] Krypton *Help pages on K400/K600 : Hardware & software guide*, Krypton, *User manuals*, Leuven, Belgium, Leuven(2003)
- [16] Krypton *Help pages on DMM-Modular*, Krypton, *User manuals*, Leuven, Belgium, Leuven(2003)
- [17] R. C. Dorf, R. H. Bishop, *Modern Control Systems, eight edition*, Addison-Wesley, *Menlo Park, CA*, Menlo Park(1998), ISBN 0-201-32677-9

